Pressure Cell Assisted Solution Characterization of Galactomannans. 3. Application of Analytical Ultracentrifugation Techniques

Trushar R. Patel,[†] David R. Picout,[‡] Simon B. Ross-Murphy,*[,‡] and Stephen E. Harding[†]

NCMH Laboratory, School of Biosciences, University of Nottingham, Sutton, Bonington LE12 5RD, and King's College London, Franklin-Wilkins Building, 150 Stamford Street, Waterloo, London SE1 9NH, United Kingdom

Received July 13, 2006; Revised Manuscript Received September 22, 2006

The pressure heating cell approach previously applied to galactomannans in two earlier studies is now used to prepare samples for characterization using the analytical ultracentrifuge. Sedimentation velocity data were obtained for both guar gum and locust bean gum samples. These were compared to our earlier light scattering and intrinsic viscosity measurements on samples prepared using identical temperature and pressure profiles. A number of methods were then employed to obtain chain persistence lengths, including the Hearst−Stockmayer and Bohdanecky wormlike chain approaches. These results were compared to earlier results obtained using methods appropriate for excluded volume coil and rodlike chains, respectively.

Introduction

Early published studies of the conformation and flexibility of water-soluble polymers, especially including polysaccharides, were often flawed by the use of inappropriate solution preparation techniques. This may be because the initial hydration steps were poorly considered, or that for many such systems obtaining "molecularly dispersed" solutions is far from trivial. This can give incorrect values for the solution concentration, which in turn lead to significant errors for the "molecular" size and shape, from dilute solution viscosity and light scattering measurements. With the latter technique the presence of incompletely dissolved material can generate results that are either not interpretable or physically improbable. This was, of course, known for many years and why, historically, the best characterization data for polysaccharides were made either in nonaqueous solution or on chemically derivatized materials. However, such approaches do raise questions about the applicability of such results to the original water-soluble sample.

A number of approaches have been adopted to try and reduce this effect; of these perhaps the earliest was the use of an alkali to both dissolve and help disperse (by charge−charge repulsion) polysaccharides. This technique originally applied to amylose[1] has subsequently been used with some effect for cereal β-glucans[2] and galactomannans.[3] Another technique is to employ a sealed vessel containing the solution heated to above 100 °C either with an oil bath or in a microwave. This was the approach originally pursued by German workers, in particular Vorwerg, Radosta, and Burchard, to produce starch solutions[4,5] and subsequently by Burchard and one of the present authors to produce solutions of a leguminous xyloglucan, detarium gum.[6,7]

Further equipment improvements can, and have, been made by prepressurizing the sealed vessel to varying extents and also changing the maximum temperature. In our earlier studies[8−10] a combination of gas overpressures (up to 10 bar) and higher temperatures (>100 °C) was found to give adequate dispersal, albeit prolonged treatment also induced chain scission. This procedure was first employed for galactomannan polymers in two of these studies.[8,9]

Galactomannans are widely used in the food, pharmaceutical, oil recovery, paint, and textile industries as thickeners and stabilizers. They are neutral polysaccharides easily harvested and extracted from the seeds of some leguminous plants. Structurally they are a family consisting of a $\beta(1\rightarrow4)$-D-mannose backbone to which D-galactose residues are attached by $\alpha(1\rightarrow6)$ links (Figure 1). Specific galactomannans are distinguished by their mannose to galactose or "M/G" ratios, and various properties of the galactomannans of major industrial importance, guar gum (GG) and locust bean gum (LBG), were considered in the first two papers of this series.[8,9] In these papers the characterization described was carried out using dilute solution capillary intrinsic viscosity, $[\eta]$, and SEC−MALLS (size exclusion chromatography coupled to multiangle laser light scattering) measurements.

In this work, the application of different high temperature (up to 160 °C) and nitrogen overpressure (typically 4 bar at 20 °C) treatments produced a series of fractions of different weight average molecular weights, M_w, for each galactomannan.

Subsequent analysis was in terms of the well-known Mark−Houwink−Sakurada and Flory relations, respectively:

$$[\eta] = K' M_w^{\alpha} \quad (1)$$

$$R_g = K'' M_w^{\nu} \quad (2)$$

From these data, and analyses in terms of (one of the) models for determining unperturbed dimensions, the so-called Burchard−Stockmayer−Fixman[11,12] or "BSF" plot of $[\eta]/M_w^{1/2}$ versus $M_w^{1/2}$, we produced estimates of the persistence length L_p for galactomannans of 3−4 nm. For polysaccharides, this compares to ~2 nm for a very flexible coil (e.g., pullulan, a linear $\alpha(1\rightarrow6)$-based glucan with a high degree of conforma-

* To whom correspondence should be addressed. Phone: +44 (0) 20 7848 4081. Fax: +44 (0) 20 7848 4082. E-mail: simon.ross-murphy@kcl.ac.uk.

[†] University of Nottingham.

[‡] King's College London.

10.1021/bm060674n CCC: $33.50
Published on Web 11/15/2006

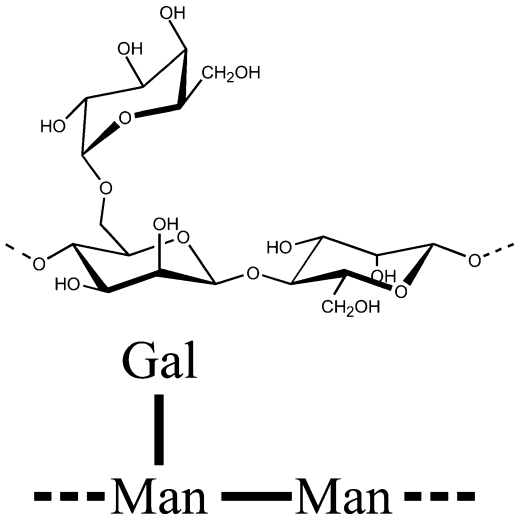

Figure 1. Galactomannan structure.

tional freedom) to ~200 nm for a "rigid rod" (e.g., schizophyllan and scleroglucan, triple-helical $\beta(1\rightarrow3)$-glucans).

Values found for the exponents α and ν were consistent with those of essentially linear coil-like macromolecules with some excluded volume, with $\alpha \approx 0.75$ and $\nu \approx 0.55$. Again, within experimental error, these values were independent of the degree of galactose substitution.

To some this is, of course, no surprise, but it appears distinctly different values are still being measured and published. For example, Wientjes et al., in their work on guar, found $\alpha \approx 1.05$;[13] this value would suggest that guar (and presumably other galactomannans) are not coil-like macromolecules, but instead are appreciably stiffened. In an earlier paper we attributed this discrepancy to a small amount of ill-dispersed material in their "solutions".[9] Subsequent careful work by Lefebvre and Doublier has confirmed this to be the case.[14]

In the present work, the final part of this trilogy, we extend and broaden these investigations by, for the first time, applying the technique of analytical ultracentrifugation to pressure cell heated samples. In particular, we investigate the homogeneity of preparations using sedimentation velocity analysis to obtain distributions of the weight average sedimentation coefficient from sedimentation velocity analysis measured at 20 °C, $s_{20,w}$, where the subscript "20,w" means corrected to standard solvent conditions (namely, the density and viscosity of water at 20.0 °C). Modal (or peak maximum) $s_{20,w}$ values, obtained from a series of concentrations, are extrapolated to zero concentration to eliminate the effects of nonideality to yield $s_{20,w}^{\circ}$. This then allows us to employ a different relationship, viz.

$$s_{20,w}^{\circ} = K''' M_w^{\ b} \tag{3}$$

and examine its significance.

Materials and Methods

Both the sample source and batches of the GG and LBG galactomannans, and the treatments employed, are the same as those reported in parts 1 and 2 of this series.[8,9] Purified samples from commercial food grade guar gum flours of different average molecular weight, namely, M30, M90, and M150 (Meyprogat range, Meyhall Chemicals A.G., Kreuzlingen, Switzerland, now part of the Danisco Group, Copenhagen, Denmark) were used in all experiments, along with locust bean gum M175 (also from Meyhall Chemicals A.G.). Both samples had been purified from the flour using an isolation procedure devised by Girhammar and Nair[15] and modified by Rayment et al.[16] to allow complete hydration of the guar gum sample. The moisture contents of the extracted polymers were determined by incubation overnight in an oven at 103 °C to a constant weight. Freeze-drying was carried out using an Ehrist ALPHA I-5 freeze-dryer [DAMON/IEC (UK) Ltd.], and the samples were stored in a desiccator until use.

The dissolution and heat−pressure procedures were as follows: dispersions were prepared by adding known weights of a freeze-dried sample of the purified galactomannan to deionized water at 50 °C, containing ~0.02% sodium azide, to give final solution concentrations of 0.5−0.75 mg/mL. As the dry powder was added, the dispersion was stirred and the temperature was raised to 80 °C. The solutions were subsequently left covered overnight, with stirring, at room temperature to facilitate hydration of the sample. A 30 mL sample of this dispersion was then added to the reaction chamber of a pressure/heating cell (HEL Ltd., Barnet, Herts, U.K.). These solutions were then subjected to a range of temperature and pressure conditions between 70 and 160 °C. In some experiments, after the reaction chamber had reached 50 °C, it was pressurized (3−12 bar) using N_2. The processing conditions were applied for a range of times from 10 min to 2 h. After this the cell was allowed to cool to room temperature, and aliquots were removed and immediately transferred to the ultracentrifuge preparation area.

Because the pressure cell temperature and agitation regime is computer controlled, it is readily reproduced and reproducible; however, as a further check on the degradation route, light scattering measurements of selected samples/conditions were repeated following the procedures described in the earlier papers. Again, the SEC system used consisted of a Jasco HPLVC pump, a guard column, and TSK G6000 and G4000 columns connected in series. A DAWN-DSP multiangle laser light scattering detector and an Optilab 903 refractometer (Wyatt Technologies, Santa Barbara, CA) were used for light scattering intensity[17] and concentration detection, respectively. Results obtained (not shown) were in agreement with past results, but since the novelty of this study resides in the ultracentrifuge results, in the analyses below, we have utilized our previously published data for M_w and R_g. We also discuss the implications of the strategy below.

Sedimentation Velocity Analysis

A series of sedimentation velocity experiments were performed using a Beckman (Palo Alto, CA) Optima XL-I analytical ultracentrifuge equipped with Rayleigh interference optics and an automatic on-line data capture system.[18] Standard 12 mm double-sector cells with sapphire windows were loaded with 0.4 mL of sample and reference solvent in the appropriate channels.[19] The balanced cells were placed in an analytical four-hole rotor (An60-Ti). After time was allowed for vacuum formation and for temperature equilibration (20.0 °C), the rotor was accelerated to 40000 rev/min. Using the Rayleigh interference optical system, scans of relative concentration (in terms of fringe displacement perpendicular to the direction of sedimentation) versus radial displacement, r, from the axis of rotation were taken at 1 min intervals throughout the duration of the experiment (typically 5−6 h).

These data were analyzed using the SEDFIT procedure of Schuck and co-workers.[20,21] This involves analysis of the evolution of the whole concentration, c, versus sedimentation distance, r, and versus time, t, distribution, $c(r,t)$, in the ultracentrifuge cell, via numerical solution of the Lamm equation:

$$\frac{\partial c}{\partial t} = (1/r)\frac{\partial}{\partial r}\left[rD\frac{\partial c}{\partial r} - s\omega^2 r^2 c\right] \tag{4}$$

in which D is the translational diffusion coefficient and ω is the angular velocity.

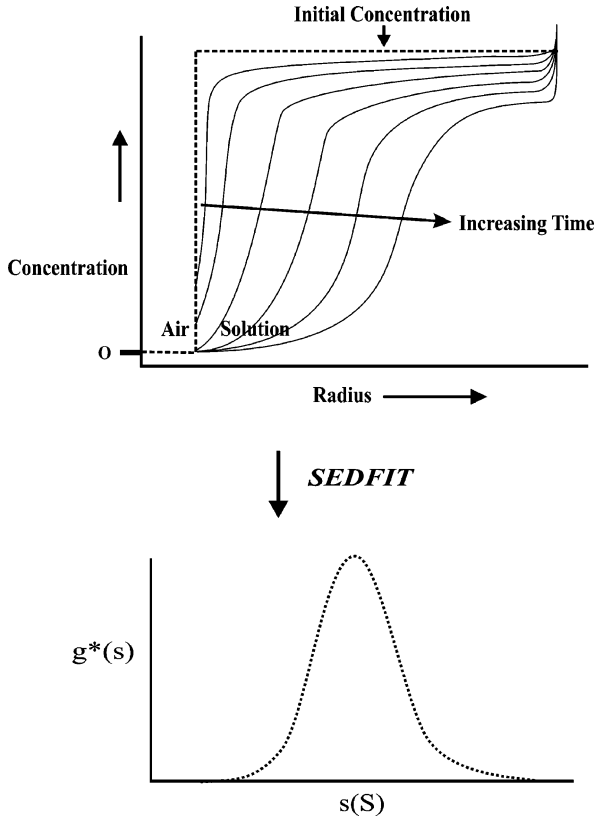

Figure 2. Schematic concentration distribution with time in the ultracentrifuge cell (top) and the $g^*(s)$ distribution after application of SEDFIT (bottom).

Two distributions of the sedimentation coefficient are generated by this procedure.[22,23] The first of these has not been corrected for diffusive broadening (or thermodynamic nonideality). This yields an "apparent" sedimentation coefficient distribution, $g^*(s)$ versus s (measured in seconds or Svedberg units, Sv = 10^{-13} s), and is approximately Gaussian in shape. Figure 2 shows schematically how a $g^*(s)$ versus s distribution is generated from a radial concentration distribution changing with time. Another distribution, "$c(s)$ versus s", where $c(s)$ is produced by the software is intended to correct for diffusion by assuming one frictional ratio applies to the whole distribution of macromolecular species. The distribution functions $g^*(s)$ and $c(s)$ both represent the population (weight fraction) of species with a sedimentation coefficient between s and $s + ds$ within their respective assumptions about diffusion and nonideality.

Although the apparent distribution may not reflect the true sedimentation coefficient distribution, the position of the peak does represent the apparent weight average sedimentation coefficient. Since measurements were made at 20.0 °C and free of added low molecular weight electrolyte, the approximation $s \approx s_{20,w}$ (sedimentation coefficient corrected to standard conditions of the viscosity and density of water at 20.0 °C) could be made. Values of $s_{20,w}$ for each galactomannan sample were then corrected for nonideality by measurement at a series of concentrations and extrapolation of the results to zero concentration using the Gralén equation[24,25] to yield $s_{20,w}°$:

$$1/s_{20,w}° = (1/s_{20,w})/(1 + k_s c) \qquad (5)$$

Here k_s (mL/g) is the sedimentation concentration dependence coefficient. Concentration extrapolations were performed by serial dilution to avoid errors of concentration accruing to our extrapolated values of $s_{20,w}°$.

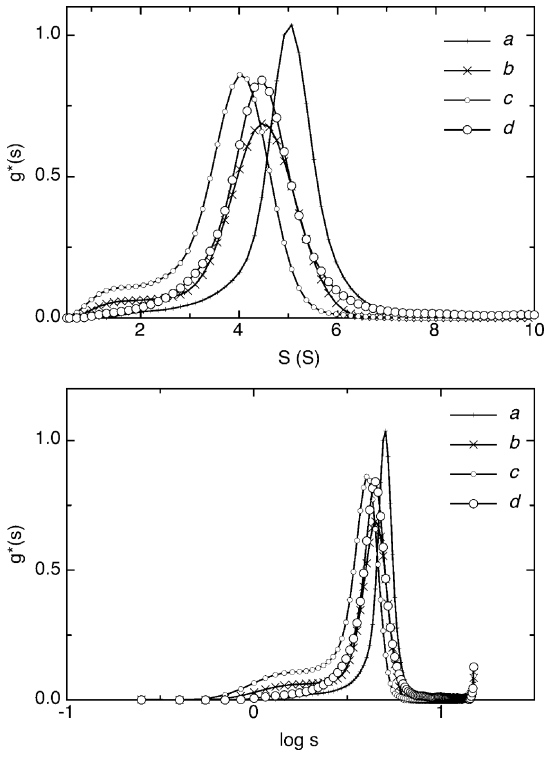

Figure 3. Extracted $g^*(s)$ distribution for guar gum plotted versus s (top) and log s (bottom). Treatments are (a) 100 °C for 10 min at 0.75 mg/mL, (b) 130 °C for 10 min at 4 bar and 0.75 mg/mL, (c) 130 °C for 60 min at 5 bar and 0.75 mg/mL, and (d) 160 °C for 10 min at 7 bar and 0.75 mg/mL.

Results

Sedimentation Data. As has been discussed by one of the present authors,[23] and mentioned above, the SEDFIT program produces both $g^*(s)$ and $c(s)$ distributions. The $c(s)$ vs s data represent an attempt to correct the width of the $g^*(s)$ distribution for diffusive effects, but the program achieves this by floating a frictional ratio parameter in the fitting procedure. The assumptions concerning the frictional ratio (i.e., one value representing the whole distribution) are considered inappropriate for polysaccharides especially when there is significant polydispersity in M_w and hence in $g^*(s)$, so this procedure is of limited use. Consequently, in the treatment below we consider only $g^*(s)$ versus s data.

All samples treated in the pressure/temperature cell yielded sedimentation coefficient distribution $g^*(s)$ vs s plots for different sedimentation times, which indicated proper dispersion and also a high degree of purity. In this section, we illustrate only certain of the factors involved rather than the full set studied; in the subsequent discussion we consider the $s_{20,w}°$ values and their significance.

First we consider the results for the GG sample illustrated in Figure 3. These results show a broad Gaussian-like distribution of s values which is essentially unimodal and with less than 5% high molecular weight material. The area under the curves is approximately constant, since this reflects the initial concentration, which in all cases was ~0.75 mg/mL. Very high molecular weight (and essentially undissolved) material would have been "pelleted out" by the time of the first scans and so would not be picked up; there was a slight hint of this with the guar (data not shown). The largest peak s value is for the sample that had the mildest treatment, in this case 100 °C for 10 min, and with a peak at around 5.2 S. Heating to 130 °C for 10

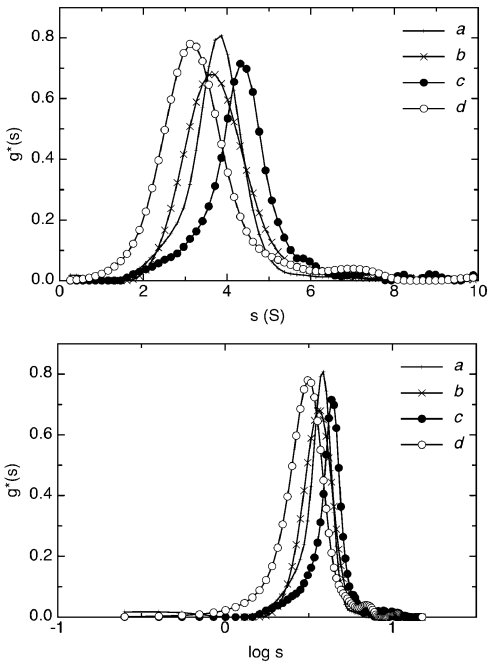

Figure 4. Same as Figure 3 but for locust bean gum. Treatments are (a) 100 °C for 10 min at 0.50 mg/mL, (b) 130 °C for 30 min at 0.50 mg/mL, (c) 130 °C for 30 min at 4 bar and 0.50 mg/mL, and (d) 160 °C for 10 min at 0.50 mg/mL.

min at 4 bar moves the peak *s* to lower values, consistent with a small amount of chain degradation. Moreover, there is evidence of the development of a second peak at lower *s* values, suggesting partial degradation but still to a relatively high M_w species. Increasing the heating time, but maintaining the temperature (and the approximate overpressure), moves the peak to still lower *s* values and also shows further development of the low *s* peak.

Interestingly, the higher temperature 160 °C run (at 7 bar) for 10 min scarcely changes the peak relative to that of the initial 130 °C run, but appears to sharpen the distribution. All of this is quite consistent with our previous observations. Plotting the data as $g^*(s)$ versus log *s* helps to accentuate the side peaks, but there is clearly very little material with $s > 10$ S.

The corresponding traces for LBG are presented in Figure 4 and show a more complex picture, which is demonstrated most clearly by examining the traces of the samples treated without N_2 overpressure. The 100 °C/10 min/0 bar overpressure trace has a peak at around 4 Sv; heating to 130 °C/30 min/0 bar reduces this marginally and slightly skews the distribution toward lower *s* values. The 160 °C/10 min/0 bar data illustrate this effect even more clearly but also show the development of "ripples" at high *s* values, consistent with accelerated aggregation. Finally, the application of overpressure (130 °C/30 min/4 bar) shifts the peak of the distribution back to higher *s* values, higher even than for the 100 °C measurement, but again with evidence of high *s* value ripples.

This trend with respect to treatment is very consistent with the previously published M_w values from light scattering. More interestingly, there is also evidence in the present measurements of "high *s* ripple" fractions. The measurements were made typically within 24 h after the pressure regime treatment, but compared to GG this is already clear evidence for reaggregation. It is well-known that LBG shows a far greater propensity for reaggregation than GG, and the kinetics of aggregation of so-called LBG cold set "gels" has been investigated in some detail.[26,27]

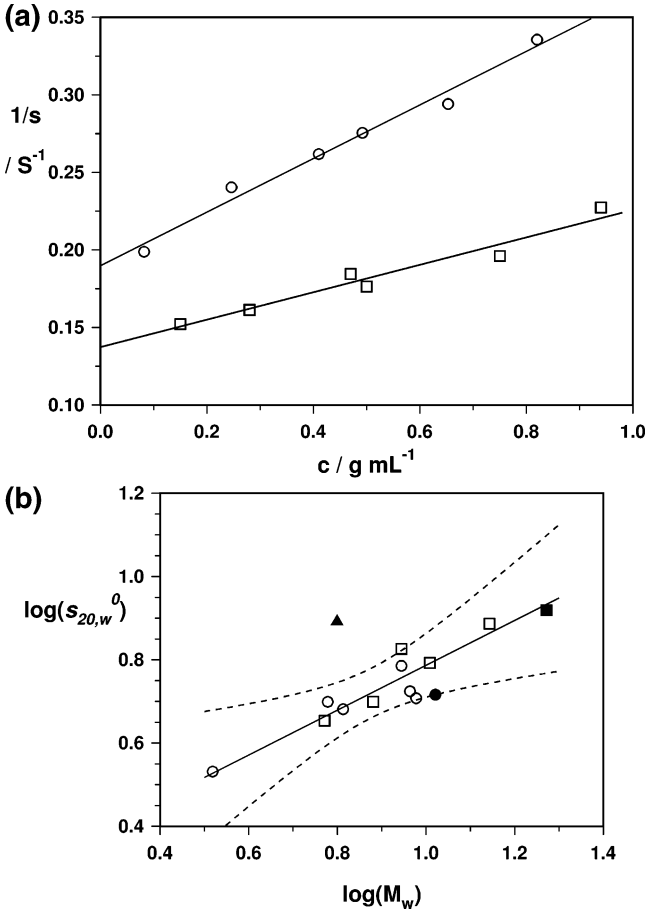

Figure 5. (a) Typical (Gralén) plots of 1/*s* versus *c* showing their linearity and the extrapolations to give intercepts $s_{20,w}^\circ$. Data are for samples heated for 10 min at 100 °C, LBG (circles) and guar (squares). (b) log $s_{20,w}^\circ$ plotted versus log M_w for guar gum (squares) and locust bean gum (circles). Filled circles and squares represent un-pressure-treated samples, and the triangle is a rogue point. Dashed lines represent 99.9% confidence intervals.

Table 1. Dependence of Measured Parameters on the Treatment Conditions for Guar Gum

treatment	$10^{-5}M_w$[a]	$R_{g,z}$[a] (nm)	$s_{20,w}^\circ$ (S)
untreated	18.7	133	8.3 ± 0.3
100 °C, 10 min	13.9	169	7.7 ± 0.2
130 °C, 10 min	8.8	105	6.7 ± 0.3
130 °C, 10 min, 4 bar	10.2	134	6.2 ± 0.3
130 °C, 60 min, 5 bar	6.3	78	7.8 ± 0.2
160 °C, 10 min, 3 bar	5.9	80	4.5 ± 0.4
160 °C, 10 min, 7 bar	7.6	87	5.0 ± 0.3

[a] From ref 8.

The $s_{20,w}^\circ$ values were extrapolated (Figure 5a) for more detailed examination and are given in Tables 1 and 2, together with the previous data for M_w and R_g. They are also plotted against M_w in Figure 5b; the squares represent data for guar gum and the circles data for LBG. Here it is important to stress that data for the latter quoted here were a quite separate sequence of nominally identical pressure cell treatments made at quite different times and in different laboratories in Nottingham and London. As is mentioned above, check remeasurements of R_g and M_w were made, and they do agree largely (but by no means perfectly) with the previously published results. However, for the purposes of the present exercise it was considered far more fruitful to use the previously published results, with any

Table 2. Dependence of Measured Parameters on the Treatment Conditions for Locust Bean Gum

treatment	$10^{-5}M_w$[a]	$R_{g,z}$[a] (nm)	$s_{20,w}°$ (S)
untreated	10.5	127	5.2 ± 0.3
100 °C, 10 min	9.2	122	5.3 ± 0.3
130 °C, 10 min	6.5	104	4.8 ± 0.2
130 °C, 30 min	6.0	104	5.0 ± 0.4
130 °C, 10 min, 4 bar	9.5	118	5.1 ± 0.3
130 °C, 30 min, 4 bar	8.8	113	6.1 ± 0.4
160 °C, 10 min	3.3	64	3.4 ± 0.2

[a] From ref 9.

accumulated errors, rather than to use the check M_w results, which would not help to verify the reliability and viability of the pressure cell method. This is, of course, a somewhat precarious policy, and there is no doubt errors are increased. However, if the pressure cell regime is to be exploited more widely, it has to be shown to be reproducible over time (in this case, years), so we feel it is a justifiable risk.

For this reason Figure 5 requires careful explanation. Following a previous protocol, we have chosen, in subsequent analysis, to ignore the data generated from the so-called (pressure cell) untreated systems, the filled square and circle, even though Figure 5 actually suggests that in this case they are quite in harmony with those for the treated samples. However, it would be inconsistent of us to now include data we earlier excluded from the analysis set, just because they now appear more satisfactory; we already know, from our earlier work, that the R_g values obtained for these samples were highly suspect. We have also excluded one point (guar gum, 130 °C, 60 min, 5 bar; filled triangle) which despite being remeasured gives an $s_{20,w}°$ value considerably outside expectation, i.e., more than 2 standard deviations away from the line. Figure 5 includes the 99.9% confidence intervals for the used data, and it is clear that this point is a "rogue". Again we could simply have not presented it here, but that would not have been consistent with the results and pressure cell treatments given in the earlier papers. In fact, as we show below, including these three points appears to *improve* the apparent slope (exponent) from this plot, albeit the error also increases. The line here represents the fit to the remaining GG and LBG data treated together, a total of 11 points, and is considered in more detail below.

Discussion

Effect of Treatment Conditions on Hydrodynamic Data. Tables 1 and 2 give the $s_{20,w}°$ values as a function of the treatment condition for guar and locust bean gum, respectively. In principle, from these it should be possible to calculate the molecular weight, but for polydisperse samples this is extremely difficult. This is because we need values for both k_s and V_s (the swollen specific volume, taking into account hydration effects). The former is given by eq 5, but for the latter a number of assumptions must be made. Instead, as discussed above, we have decided to use the current values of $s_{20,w}°$ and compare these with the previously published values of M_w and R_g given in the same two tables.

Both guar and LBG data are plotted, and the overall slope is 0.54 ± 0.07. For Θ solvent conditions, the slope of this plot, b, cf. eq 3, should be ~0.5; for good solvents it should be ~0.4. By contrast, for the case of dominant hydrodynamic interaction, corresponding values of the rigid rod and sphere limits for b are respectively 0.67 and 0.15. The slopes for the results of the two together suggest that these systems show some chain stiffness and/or poor solvent behavior. However, when treated separately, the corresponding results are 0.65 ± 0.10 and 0.43 ± 0.10, respectively, the former being close to the rod limit, the latter to representing a coil in a better than Θ solvent. In fact "better" results are obtained if we reinclude the excluded data; e.g., the slope for guar gum is reduced to 0.49 and the overall slope to 0.50, and including the rogue point makes the overall exponent a little lower still at 0.46 albeit with increased error! Overall this suggests, not surprisingly, that it is unsafe to deduce too much simply from such exponents.

Table 3. Experimental Power Law Values for Galactomannans and Corresponding Values from the Tsvetkov, Eskin, and Frenkel Relations

	guar	locust bean gum	overall
α[a]	0.70 ± 0.10	0.77 ± 0.09	0.74 ± 0.05
2 − 3b	0.05	0.68	0.38 (±0.21)
ν[a]	0.54 ± 0.05	0.57 ± 0.05	0.55 ± 0.03
(α + 1)/3	0.58	0.59	0.58 (±0.02)
b	0.65 ± 0.10	0.43 ± 0.10	0.54 ± 0.07
1 − ν	0.46	0.43	0.45 (±0.03)

[a] Data from refs 8 and 9.

Tsvetkov−Eskin−Frenkel Relations. To demonstrate this point still further, we can use our previously obtained estimates for α, eq 1, ν, eq 2, and b, eq 3, to apply the so-called Tsvetkov, Eskin, and Frenkel (TEF) relations:[28]

$$\alpha \approx 2 - 3b \tag{6}$$

$$\nu \approx (\alpha + 1)/3 \tag{7}$$

$$b \approx 1 - \upsilon \tag{8}$$

In Table 3 we have given the values of these parameters, which according to the above suggestions should be identical, within experimental error, to α, ν, and b, respectively, estimated earlier. Clearly the error bounds on the estimates suggest that any "positive" result should be regarded sceptically, and examination of the final results supports this. For example, LBG appears to follow eq 6 relatively well, whereas for GG agreement is very poor, as we might expect from earlier comments. The overall result (0.38) is "improved" only by considering the very large error (±0.21) on this estimate. TEF relationships may be useful in some circumstances, but not in the present case. We present this result simply to reinforce our earlier remarks that comparing exponents is a limited exercise.

Indeed relying simply on "scaling laws" is a poor return for the novelty and extent of the new results obtained, when we are more interested in really quantitative conformational information on the galactomannan family. To explore this further, we now consider a number of options to obtain what we would argue was the most fundamental chain parameter, the chain persistence length, L_p.

Estimates of L_p. *Hearst−Stockmayer (HS) Approach*. Although now largely of historical interest, the advantage of this method is that it only requires the sedimentation and M_w results, and not those for R_g or $[\eta]$. For fuller details, the original paper, a subsequent source (e.g., Yamakawa's classic monograph[29]), or, most usefully, a more recent update[30] should be consulted. This incorporates the Yamakawa−Fujii wormlike chain into the original HS treatment.

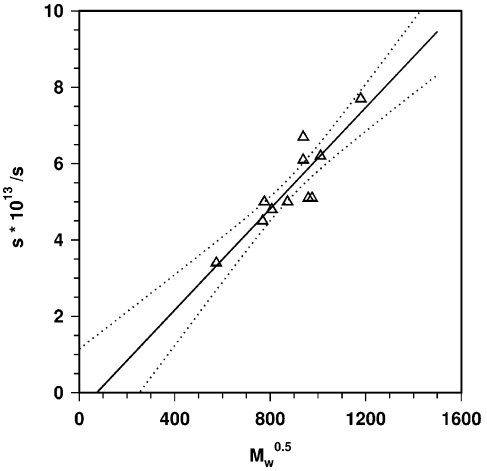

Figure 6. Hearst−Stockmayer plot for guar and LBG pressure-treated samples. Dashed lines represent 95% confidence intervals. L_p is calculated from the slope.

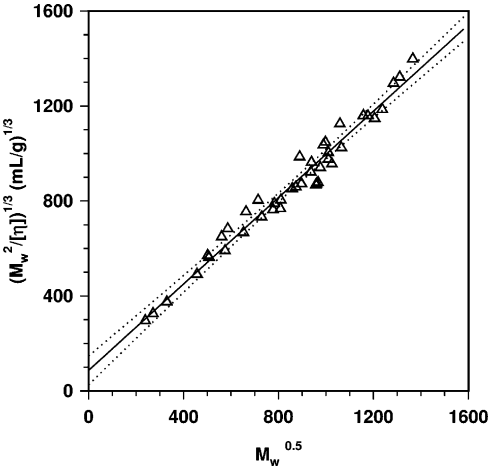

Figure 7. Bohdanecky plot for guar and LBG, including literature data. L_p is calculated from the slope.

According to the latter treatment, we can write

$$s = \frac{M(1-\bar{\nu}\rho)}{3\pi\eta N_A L}[1.843(L/2L_p)^{1/2} - \ln(d/2L_p) + 0.1382(L/2L_p)^{-1/2} + ...] \quad (9)$$

where L is the chain contour length and is given by $L = M/M_L$, with M_L the chain mass per unit length, η is the solvent viscosity, $\bar{\nu}$ is the partial specific volume, and N_A is Avogadro's number. We have to assume here, of course, that we can replace M by M_w with all that this implies.

To obtain L_p, we then plot (see Figure 6) the measured values of $s_{20,w}°$—here simply called s—versus $M_w^{0.5}$. In this plot we have again treated the LBG and GG data as coming from the same overall set; the significance of this is discussed below.

In this range, and for most purposes, it should be sufficient to truncate the series of eq 9 after one term. However, we have tried both this and a full nonlinear fit to the first three terms, although including the latter seems to contribute ∼5% overall to the series. Here we use 450 per nanometer for the mass per unit length term, M_L, a reasonable value for galactomannans.[31,32] The value of M_L should, of course, be marginally greater for the more substituted GG than for LBG, if they are similarly flexible—something we feel we have already established—but we chose to neglect this effect. The calculated values[9] of the residue molecular weights, m_r, for guar and LBG are 267 and 223, respectively; i.e., they differ by ∼20%.

The results are quite encouraging; using 0.613 mL/g for the partial specific volume and 1 cP (= 1 mPa s) for the viscosity of water, we obtain 8.1 ± 1.1 nm for L_p from the linear plot (first term), and 8.8 ± 0.8 nm from a fit to all three terms. This contrasts, not at all unreasonably, with our previously published values of ∼4 nm from the Burchard−Stockmayer−Fixman method[11,33] and ∼8 nm from the so-called Hearst method[34] for the total set which included GG, LBG, and the still less substituted galactomannan tara gum. This difference, large though it may appear, is because the assumptions behind these methods are themselves quite different; subsequently, we use this opportunity to discuss this in more detail. However, even this clearly demonstrates the observation that, using the BSF procedure, lower persistence lengths are obtained than using the Hearst model. One aspect of this which is ripe for reconsideration is the reliability of different extrapolation methods for unperturbed dimensions and persistence length, so we now employ the Bohdanecky method,[35] which should give intermediate results, to see how this compares.

For consistency, we have also recalculated the values from BSF and Hearst, but now employing the assumption that the residue weight, m_r, and also M_L are independent of the substitution extent. This assumption does tend to alter the results from earlier studies somewhat, although it does not take L_p values outside previously established error bounds. As we mentioned above, the difference in the m_r values of GG and LBG is ∼20%, so the error is ±10%. Although this may seem a large difference in absolute terms, that between different extrapolation methods (see below) is certainly larger than this.

Bohdanecky method.[35] This is a method which is becoming among the most popular, particularly for semiflexible polymers, and has been applied to charged polysaccharides including xanthan,[36,37] sodium hyaluronate,[38] and alginate[39] and certain neutral polysaccharides such as cereal β-glucans.[40] It employs the rather user-unfriendly Yamakawa−Fujii (YF) wormlike chain theory, but one of Bohdanecky's most valuable contributions was to tabulate terms in the YF model and therefore make it much easier to apply. In its simplest form, the Bohdanecky method involves plotting $(M^2/[\eta])^{1/3}$ versus $M^{1/2}$, from which L_p can be found from the slope, using eq 10 and tabulated values of B_0:

$$\left(\frac{M^2}{[\eta]}\right)^{1/3} = A_\eta + B_0\Phi^{-1/3}\left(\frac{2L_p}{M_L}\right)^{-1/2} M^{1/2} \quad (10)$$

Figure 7 illustrates this plot for the same 11 data points we have used, for example, in Figure 6, together with a range of other data for guar samples we used in earlier studies. This includes that of Beer and co-workers[41]—which extends to lower M_w—and the widely cited, but early, data of Robinson et al.[42] In total we have 42 data points, but the Bohdanecky plot is still gratifyingly linear. Using Flory's Φ for infinite nondraining coils, 2.86×10^{-23} mol^{-1}, we obtained $L_p = 6.3 \pm 0.2$ nm. With this plot deviations tend to occur only when the number (n_k) of Kuhn lengths ($=2L_p$) in the chain contour length ($=M_w/M_L$) is <∼5, i.e., in this case when $M_w < \sim 3 \times 10^4$ and the chain approaches a rod limit. Even with the Beer data we are still above this.

BSF and Hearst Methods and the Influence of Excluded Volume. Using the same data set and treating it in the very same way, i.e., without tara gum and with no correction for the different m_r values for guar and LBG, we can also extract L_p from the BSF and Hearst methods. In the former, L_p is extracted

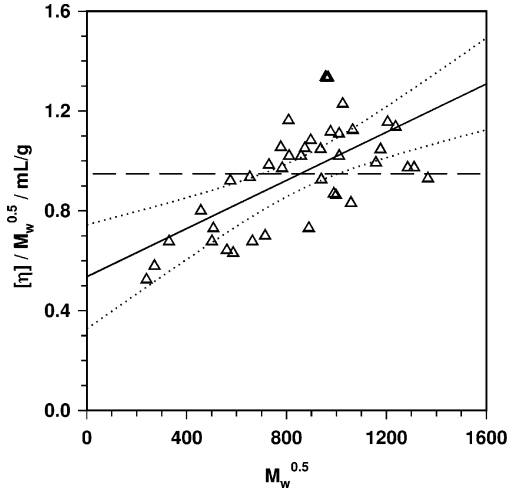

Figure 8. BSF plot for guar and LBG, including literature data. The horizontal dashed line represents the best θ (=0) fit to these points. L_p is calculated from the intercept(s).

from the intercept and for the latter from the slope of the appropriate plots. Corresponding values are 4.1 ± 0.6 nm (Figure 8) and 7.9 ± 0.8 nm, respectively (plot not shown).

The order of the above L_p values, i.e., BSF < Bohdanecky < Hearst, corresponding to the different models, random flight chain, wormlike chain, and rodlike chain, is precisely as we would expect. The HS value, also for a wormlike chain, is marginally the largest at ~8.5 nm, but is based on different assumptions. Overall, the agreement between different methods is gratifying particularly since "the evaluation of the stiffness of a macromolecular chain through the persistence length is a very delicate task".[38]

The BSF approach assumes that at low enough M_w the chain becomes Gaussian, i.e., that long-range excluded volume correlations disappear. By contrast, the Hearst model assumes that the chain approaches a rodlike limit and neglects excluded volume effects. The Bohdanecky and the modified Hearst−Stockmayer approaches also ignore excluded volume effects, and here both treat the chain stiffness as coming from the intrinsic properties of a wormlike chain. Clearly the neglect of excluded volume effects, if they are actually present, would result in slightly greater values of L_p. Another way of demonstrating this is to assume that the BSF line actually has a slope of zero—i.e., the chain has no excluded volume. Under this, albeit simplistic, assumption, the value of the BSF L_p increases to 6.1 ± 0.7 nm, significantly closer to those from the other treatments and statistically identical to the Bohdanecky result (Figure 8, dashed line).

Another way of testing this effect is to estimate the limit above which excluded volume behavior should appear. According to Fujita,[43] this should be when $n_k > 50$, so that the chain contour length, M_w/M_L, has to be around 100× greater than L_p. Assuming for the moment that $L_p \approx 6$ nm and $M_L \approx 450$, $M_w \approx 100 \times 6 \times 450 = 2.25 \times 10^5$ so that $M^{0.5} > \sim 520$. In our case >90% of the data satisfy this condition. More recently, a still lower limit, in the region of $10L_p$ to $20L_p$, has been suggested by Norisuye and co-workers for semiflexible polymers.[44] In this case $M^{0.5} > \sim 150$; all our data lie within this extended region.

Despite the above comments, the overall range of ~2× (from BSF to HS) might still appear to some rather large, so we suggest that, in the future, especially for such biopolymer systems, where absolute sample quality cannot be guaranteed, the values cited should be appended by the method. For example, "we find that, *using the Bohdanecky method*, L_p is 6.3 ± 0.2 nm".

Arguably the most absolute methods for determining L_p, in that they make no assumptions about hydrodynamics, are those that simply analyze the shape of the angular dependence of the zero concentration scattered light intensity using, for example, the Benoit−Doty method extended to polydisperse chains, and employing the so-called Kratky method.[45] This has proved of great value for extremely persistent chains such as xanthan, $L_p \approx 120$ nm.[46] However, for the present systems, when R_g values are mostly <~120 nm, the wavelength λ is 628/1.333 nm, and the maximum range of the relevant parameter u ($=R_g/[4\pi/\lambda]$) is nearly always $0 < u < \sim 3$, the method is not so useful and was not attempted here.

Concluding Remarks

This study confirms the importance of ensuring adequate dispersion of polysaccharides prior to hydrodynamic or other scattering characterizations and, more importantly, how we can use modern analytical ultracentrifuge procedures to assess that dispersion. It is worth remarking that sedimentation methods are not as affected by incomplete dispersal of macromolecules compared with viscometry and light scattering measurements. This is first because overestimates of the macromolecular concentration do not normally influence the calculated value for $s_{20,w}°$ (unlike $[\eta]$ and R_g from viscometry and light scattering, respectively) and second because any incompletely dispersed material is usually quickly removed by the centrifugal field.[23] We would therefore encourage its extended exploitation as a member of the suite of techniques for studying polysaccharide chain flexibility.

Acknowledgment. We thank the United Kingdom Biotechnology and Biological Sciences Research Council for providing support for this study (Grant Reference 29/D10446). T.R.P. is the recipient of a University of Nottingham New Route Scholarship.

References and Notes

(1) Doppert, H. L.; Staverman, A. J. *J. Polym. Sci., Part A-1* **1966**, *4*, 2373.
(2) Li, W.; Wang, Q.; Cui, S. W.; Huang, X.; Kakuda, Y. *Food Hydrocolloids* **2006**, *20*, 361.
(3) Goycoolea, F. M.; Morris, E. R.; Gidley, M. J. *Carbohydr. Polym.* **1995**, *27*, 69.
(4) Vorwerg, W.; Radosta, S. *Macromol. Symp.* **1995**, *99*, 71.
(5) Aberle, T.; Burchard, W.; Vorwerg, W.; Radosta, S. *Starch/Staerke* **1994**, *46*, 329.
(6) Wang, Q.; Ellis, P. R.; Ross-Murphy, S. B.; Reid, J. S. G. *Carbohydr. Res.* **1996**, *284*, 229.
(7) Wang, Q.; Ellis, P. R.; Ross-Murphy, S. B.; Burchard, W. *Carbohydr. Polym.* **1997**, *33*, 115.
(8) Picout, D. R.; Ross-Murphy, S. B.; Errington, N.; Harding, S. E. *Biomacromolecules* **2001**, *2*, 1301.
(9) Picout, D. R.; Ross-Murphy, S. B.; Jumel, K.; Harding, S. E. *Biomacromolecules* **2002**, *3*, 761.
(10) Picout, D. R.; Ross-Murphy, S. B.; Errington, N.; Harding, S. E. *Biomacromolecules* **2003**, *4*, 799.
(11) Burchard, W. *Makromol. Chem.* **1963**, *59*, 16.
(12) Stockmayer, W. H.; Fixman, N. J. *J. Polym. Sci.* **1963**, *C1*, 147.
(13) Wientjes, R. H. W.; Duits, M. H. G.; Jongschaap, R. J. J.; Mellema, J. *Macromolecules* **2000**, *33*, 9594.
(14) Lefebvre, J.; Doublier, J. L. In *Polysaccharides: Structural Diversity and Functional Versatility*; Dimitriu, S., Ed.; Marcel Dekker: New York, 2005; p 357.
(15) Girhammar, U.; Nair, B. M. *Food Hydrocolloids* **1992**, *6*, 285.
(16) Rayment, P.; Ross-Murphy, S. B.; Ellis, P. R. *Carbohydr. Polym.* **1995**, *28*, 121.
(17) Wyatt, P. J. *Anal. Chim. Acta* **1993**, *272*, 1.

(18) Giebeler, R. In *Analytical Ultracentrifugation in Biochemistry and Polymer Science*; Harding, S. E., Ed.; Royal Society of Chemistry: Cambridge, U.K., 1992; p 16
(19) Scott, D. J.; Harding, S. E.; Rowe, A. J. *Analytical Ultracentrifugation Techniques and Methods*; The Royal Society of Chemistry: Cambridge, 2005.
(20) Schuck, P. *Biophys. J.* **1998**, *75*, 1503.
(21) Dam, J.; Schuck, P. In *Numerical Computer Methods, Part E*; Brand, M. L. J., Ed.; Academic Press: New York, 2004; p 185.
(22) Harding, S. E. *Carbohydr. Res.* **2005**, *340*, 811.
(23) Harding, S. E. *Adv. Polym. Sci.* **2005**, *186*, 211.
(24) Gralen, N. Sedimentation and Diffusion Measurements On Cellulose And Cellulose Derivatives. Ph.D. Thesis, University of Uppsala, 1944.
(25) Schachman, H. K. *Ultracentrifugation in Biochemistry*; Academic Press: New York, 1959.
(26) Richardson, P. H.; Norton, I. T. *Macromolecules* **1998**, *31*, 1575.
(27) Richardson, P. H.; Clark, A. H.; Russell, A. L.; Aymard, P.; Norton, I. T. *Macromolecules* **1999**, *32*, 1519.
(28) Tsvetkov, V. N.; Eskin, V.; Frenkel, S. *Structure of Macromolecules in Solution*; Butterworths: London, 1970.
(29) Yamakawa, H. *Modern Theory of Polymer Solutions*; Harper and Row: New York, 1971.
(30) Freire, J. J.; Garcia de la Torre, J. In *Analytical Ultracentrifugation in Biochemistry and Polymer Science*; Harding, S. E., Ed.; Royal Society of Chemistry: Cambridge, 1992; p 346.
(31) Pavlov, G. M.; Rowe, A. J.; Harding, S. E. *Trends Anal. Chem.* **1997**, *16*, 401.
(32) Pavlov, G. M.; Harding, S. E.; Rowe, A. J. *Prog. Colloid Polym. Sci.* **1999**, 76.
(33) Stockmayer, W. H.; Fixman, N. J. *J. Polym. Sci.* **1963**, *C1*, 147.
(34) Kovar, J.; Fortelny, I.; Bohdanecky, M. *Makromol. Chem.* **1979**, *180*, 1749.
(35) Bohdanecky, M. *Macromolecules* **1983**, *16*, 1483.
(36) Sato, T.; Norisuye, T.; Fujita, H. *Macromolecules* **1984**, *17*, 2696.
(37) Sato, T.; Norisuye, T.; Fujita, H. *Polym. J.* **1984**, *16*, 341.
(38) Mendichi, R.; Doltes, L.; Schieroni, A. G. *Biomacromolecules* **2003**, *4*, 1805.
(39) Vold, I. M. N.; Kristiansen, K. A.; Christensen, B. E. *Biomacromolecules* **2006**, *7*, 2136.
(40) Gomez, C.; Navarro, A.; Manzanares, P.; Horta, A.; Carbonell, J. V. *Carbohydr. Polym.* **1997**, *32*, 17.
(41) Beer, M. U.; Wood, P. J.; Weisz, J. *Carbohydr. Polym.* **1999**, *39*, 377.
(42) Robinson, G.; Ross-Murphy, S. B.; Morris, E. R. *Carbohydr. Res.* **1982**, *107*, 17.
(43) Fujita, H. *Macromolecules* **1988**, *21*, 179.
(44) Norisuye, T.; Tsuboi, A.; Teramoto, A. *Polym. J.* **1996**, *28*, 357.
(45) Burchard, W. In *Physical Techniques for the Study of Food Biopolymers*; Ross-Murphy, S. B., Ed.; Blackie Academic and Professional: Glasgow, U.K., 1994; p 151.
(46) Coviello, T.; Kajiwara, K.; Burchard, W.; Dentini, M.; Crescenzi, V. *Macromolecules* **1986**, *19*, 2826.

BM060674N